

SLIDING MODE CONTROL OF A DOUBLY FED INDUCTION GENERATOR FOR WIND TURBINES

MOHAMED ADJOUJ, MOHAMED ABID, ABDELGHANI AISSAOUI,
YOUCEF. RAMDANI, HOURIA BOUNOUA

Key words: Doubly fed induction generator, Sliding mode control, Vector control, Power control.

This work presents a sliding mode control (SMC) applied to a doubly fed induction generator (DFIG) used in the wind energy conversion system (WECS). This technique finds its strongest justification to the problem of use of a robust non-linear control law for the model uncertainties. The objective is to apply this control to command independently the active and the reactive power generated by the asynchronous machine which is decoupled by the orientation of the flux. The obtained simulation results show the increasing interest of a such control in the electric systems

1. INTRODUCTION

The evolution of the wind electrical energy production does not cease increasing since 1980. It is the source which progresses most quickly and, its development is important considering the diversity of the exploitable zones and the relatively interesting cost [1]. Moreover, this energy world potential is estimated to be very important and represents a very promising energy arising.

In order to be able to test control laws of a wind system, it is essential to have a simulation tools able to model the whole energy transformation chain and to test its performances [2].

In this paper, first, a wind turbine system is presented and its characteristics are depicted to estimate its dynamics and performances in different operating conditions. Then, a SMC of the DFIG used to control independently the powers is proposed and tested on a wind turbine equipped with a DFIG of 10 kW.

2. WIND TURBINE CHARACTERISTICS

A total scheme of a wind energy conversion system connected to the electrical power grid is described by Fig. 1.

IRECOM Laboratory, Electrotechnical Department, Sidi Belabbes University, Algeria, Moh,
E-mail_adjoudj@yahoo.fr

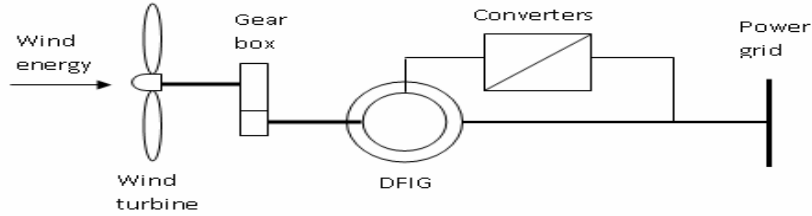


Fig. 1 – Scheme of energy transformation chain.

The power available on the wind turbine is given by [3–4]

$$P = \frac{1}{2} \rho C_p S v^3, \quad (1)$$

where: ρ – air density, S – turbine area, v – wind speed, C_p – power coefficient.

For the wind turbine, the power coefficient C_p , depending at the same time on the wind speed and the turbine rotating speed, is defined between 0.35 and 0.5.

A wind turbine is dimensioned to develop on its shaft a nominal power P_n , obtained from the nominal wind speed v_n . When the wind speed is higher than v_n , the wind turbine must modify its parameters in order to avoid the mechanics destroy [4–5].

Beside the nominal speed v_n , it is also specified the starting speed v_d where the wind turbine starts producing energy and, the maximum wind speed v_{max} where the turbine does not convert any more the wind energy. The aerodynamic control principle that limits the power extracted from the turbine at nominal output power value of the generator is based on “pitch” system [4–5] to adjust the blades lift force at the wind speed, to maintain the power appreciably constant.

The interest of this control appears by observing the characteristics on the diagram in Fig. 2.

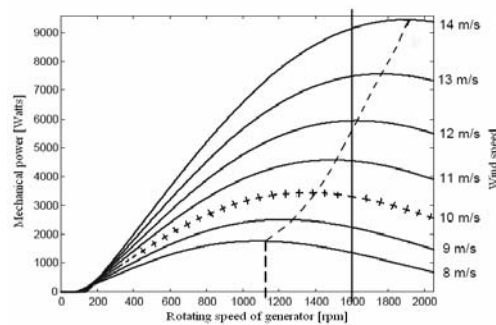


Fig. 2 –Turbine power versus its rotating speed, for various wind speeds.

2.1. GENERATOR MODELING

The generator chosen for the wind energy transformation is the doubly fed induction generator (DFIG) [6–7]. Moreover, a DFIG controlled by the rotor is used with a speed variation range limitation of $\pm 50\%$ of the nominal speed. This choice permits the use of only one converter dimensioned for an output power of about 25 to 30% of the nominal output. It will be thus less bulky, less expensive and will require a less cumbersome cooling system [8].

The modeling of the DFIG is described in the d - q Park reference frame. The following equation system describes the total generator model.

$$\begin{aligned}
 V_{ds} &= R_s I_{ds} + \frac{d\phi_{ds}}{dt} - \dot{\theta}_s \phi_{qs} \\
 V_{qs} &= R_s I_{qs} + \frac{d\phi_{qs}}{dt} + \dot{\theta}_s \phi_{ds} \\
 V_{dr} &= R_r I_{dr} + \frac{d\phi_{dr}}{dt} - \dot{\theta}_r \phi_{qr} \\
 V_{qr} &= R_r I_{qr} + \frac{d\phi_{qr}}{dt} + \dot{\theta}_r \phi_{dr}
 \end{aligned}
 \quad
 \begin{aligned}
 \phi_{ds} &= L_s I_{ds} + M I_{dr} \\
 \phi_{qs} &= L_s I_{qs} + M I_{qr} \\
 \phi_{dr} &= L_r I_{dr} + M I_{ds} \\
 \phi_{qr} &= L_r I_{qr} + M I_{qs}
 \end{aligned}
 \quad (2)$$

where: s/r are stator/rotor subscript; V/I – voltage/current; ϕ – flux; R – resistance; LM – inductance mutual; σ – leakage coefficient, ($\sigma = 1 - M^2 / L_s L_r$); θ_r / θ_s – rotor/stator position; $\dot{\theta}_r / \dot{\theta}_s$ – rotor/stator electrical speed.

3. CONTROL STRATEGY OF THE DOUBLY FED INDUCTION GENERATOR

For obvious reasons of simplifications, the d - q reference frame related to the stator spinning field pattern and a stator flux aligned on the d -axis were adopted [7–9]. Moreover, the stator resistance can be neglected since it is a realistic assumption for the generators used in the wind turbine.

The DFIG is controlled by the rotor voltages via an inverter. It is an independent control of active and reactive powers. In the d - q reference frame, in an asynchronous generator stator, the active power P_s and reactive power Q_s are:

$$P_s = V_{ds} I_{ds} + V_{qs} I_{qs}, \quad (3)$$

$$Q_s = V_{qs} I_{ds} - V_{ds} I_{qs}. \quad (4)$$

The adaptation of these equations to the simplifying assumptions gives

$$P_s = -V_s \frac{M}{L_s} I_{qr}, \quad (5)$$

$$Q_s = -V_s \frac{M}{L_s} I_{qr} + \frac{V_s^2}{L_s \omega_s}. \quad (6)$$

$L_s \omega_s$ is the stator reactance. Equations showing the relationship between the rotor currents and voltages are established and will be applied to control the generator

$$V_{dr} = R_r I_{dr} + \left(L_r - \frac{M^2}{L_s} \right) \frac{d I_{dr}}{dt} - g \left(L_r - \frac{M^2}{L_s} \right) \omega_s I_{qr}, \quad (7)$$

$$V_{qr} = R_r I_{qr} + \left(L_r - \frac{M^2}{L_s} \right) \frac{d I_{qr}}{dt} + g \left(L_r - \frac{M^2}{L_s} \right) \omega_s I_{dr} + g \frac{M V_s}{L_s}. \quad (8)$$

Since the power grid frequency is imposed, $\dot{\theta}_r = g \omega_s$, g is the DFIG slip. From equations (5), (6), (7) and (8), a block diagram containing the rotor voltages as inputs and active and reactive stator powers as outputs, is established in Fig. 3.

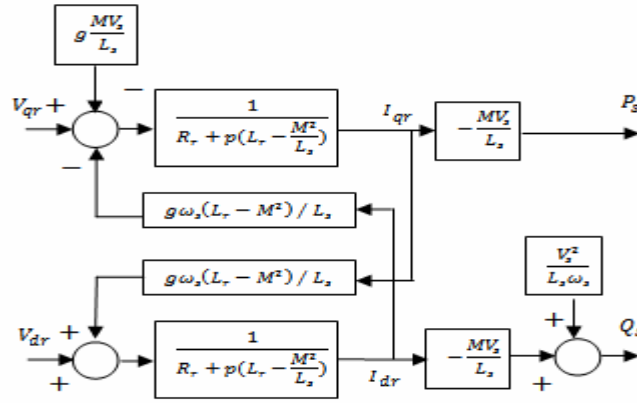


Fig. 3 – Block diagram of the generator.

The powers and the voltages are linked by a first order transfer function. Since the slip value is weak, it is possible to establish a vectoriel control, because

the influence of the coupling will remain weak and the d and q axes can be controlled separately with their own regulators.

The method used in power control consists to neglect the coupling terms and to insert an independent controller on each axe in order to control the active and reactive power independently; this method is called direct because the rotorique voltages are contolled directly by the power controllers.

4. SLIDING MODE CONTROL OF THE DFIG

The sliding mode control knows a big success these last years. It is due to the implementation simplicity and the robustness with regard to the system uncertainties and the external disturbances. The SMC consists to return the state trajectory towards the sliding surface and to develop it above, with a certain dynamics up to the equilibrium [10–11]. Its design consists mainly to determine three stages.

4.1. THE SWITCHING SURFACE CHOICE

For a non-linear system represented by the following equation:

$$\dot{\mathbf{X}} = f(\mathbf{X}, t) + g(\mathbf{X}, t) u(\mathbf{X}, t); \mathbf{X} \in \mathbb{R}^n, u \in \mathbb{R}, \quad (9)$$

where: $f(\mathbf{X}, t)$, $g(\mathbf{X}, t)$ are two continuous and uncertain non-linear functions, supposed limited.

We take the general equation to determine the sliding surface, proposed by J.J. Slotine [10], given by:

$$S(\mathbf{X}) = \left(\frac{d}{dt} + \lambda \right)^{n-1} \mathbf{e}; \quad (10)$$

$$\mathbf{e} = \mathbf{X}^d - \mathbf{X}; \quad \mathbf{X} = [x, \dot{x}, \dots, x^{n-1}]^T; \quad \mathbf{X}^d = [x^d, \dot{x}^d, \ddot{x}^d, \dots]^T, \quad (11)$$

where: \mathbf{e} – error on the signal to be adjusted, λ – positive coefficient, n – system order, \mathbf{X}^d – desired signal, \mathbf{X} – state variable of the control signal.

4.2. CONVERGENCE CONDITION

The convergence condition is defined by the Lyapunov equation [11], it makes the surface attractive and invariant

$$S(\mathbf{X})\dot{S}(\mathbf{X}) \leq 0. \quad (12)$$

4.3. CONTROL CALCULATION

The control algorithm is defined by the relation

$$u = u^{eq} + u^n, \quad (13)$$

where: u – control signal, u^{eq} – equivalent control signal, u^n – switching control term, $\text{sat}(S(\mathbf{X})/\varphi)$ – saturation function, φ – threshold width of the saturation function.

$$u^n = u^{\max} \text{sat}(S(\mathbf{X})/\varphi), \quad (14)$$

$$\text{sat}(S(\mathbf{X})/\varphi) = \begin{cases} \text{sign}(S) & \text{if } |S| > \varphi \\ S/\varphi & \text{if } |S| < \varphi \end{cases}. \quad (15)$$

5. ACTIVE POWER CONTROL

To control the power we set $n = 1$, the expression of the active power control surface becomes:

$$S(P) = (P_s^{ref} - P_s). \quad (16)$$

Taking its derivative and replacing it in the active power expression (5) we get :

$$\dot{S}(P) = \left(\dot{P}_s^{ref} + V_s \frac{M}{L_s} \dot{I}_{qr} \right). \quad (17)$$

Taking the current expression \dot{I}_{qr} from the voltage V_{qr} equation (8) and neglecting the coupling term, since the slip g is weak, we have

$$\dot{S}(P) = \left(\dot{P}_s^{ref} + V_s \frac{M}{L_s L_r \sigma} (V_{qr} - R_r I_{qr}) \right). \quad (18)$$

Replacing V_{qr} by $V_{qr}^{eq} + V_{qr}^n$, the control appears clearly in the following equation:

$$\dot{S}(P) = \left(\dot{P}_s^{ref} + V_s \frac{M}{L_s L_r \sigma} ((V_{qr}^{eq} + V_{qr}^n) - R_r I_{qr}) \right), \quad (19)$$

During the sliding mode and in steady state, we have:

$$S(P) = 0, \dot{S}(P) = 0, V_{qr}^n = 0. \quad (20)$$

The equivalent control amount V_{qr}^{eq} is found from the previous equations and written as:

$$V_{qr}^{eq} = -\dot{P}_s^{ref} \frac{\sigma L_s L_r}{V_s M} + R_r I_{qr}, \quad (21)$$

During the convergence mode, so that the condition $S(P)\dot{S}(P) \leq 0$ is verified, we set:

$$\dot{S}(P) = -V_s \frac{M}{\sigma L_s L_r} V_{qr}^n, \quad (22)$$

and consequently, the switching term is given by

$$V_{qr}^n = KV_{qr} \text{sign}(S(P)), \quad (23)$$

To verify the system stability condition, the parameter KV_{qr} must be positive.

To reduce any possible overshoot of the reference voltage V_{qr} , it is often useful to add a voltage limiter

6. REACTIVE POWER CONTROL

The same procedure as the active power is followed replacing P by Q and taking into account the reactive power expression (6) to get

$$\dot{S}(Q) = \left(\dot{Q}_s^{ref} - \left(-V_s \frac{M}{L_s} \dot{I}_{dr} \right) \right). \quad (24)$$

The expression of the current \dot{I}_{dr} is taken from the voltage V_{dr} equation (7)

$$\dot{S}(Q) = \left(\dot{Q}_s^{ref} + V_s \frac{M}{L_s L_r \sigma} (V_{dr} - R_r I_{dr}) \right), \quad (25)$$

Replacing V_{dr} by $V_{dr}^{eq} + V_{dr}^n$, the control appears clearly in the following equation:

$$\dot{S}(Q) = \left(\dot{Q}_s^{ref} + V_s \frac{M}{L_s L_r \sigma} \left((V_{dr}^{eq} + V_{dr}^n) - R_r I_{dr} \right) \right), \quad (26)$$

After computation, the equivalent control amount V_{dr}^{eq} is found to be as follows:

$$V_{dr}^{eq} = -\dot{Q}_s^{ref} \frac{\sigma L_s L_r}{V_s M} + R_r I_{dr}, \quad (27)$$

and, the switching term is given by

$$V_{dr}^n = KV_{dr} \text{sign}(S(Q)). \quad (28)$$

To verify the system stability condition, the parameter KV_{dr} must be positive.

To reduce any possible overshoot of the reference voltage V_{dr} , it is often useful to add a voltage limiter.

7. SIMULATION RESULTS

Simulation is done to illustrate the performances of the sliding mode control applied to the DFIG. A bloc diagram is proposed in Fig. 4 to control the whole system

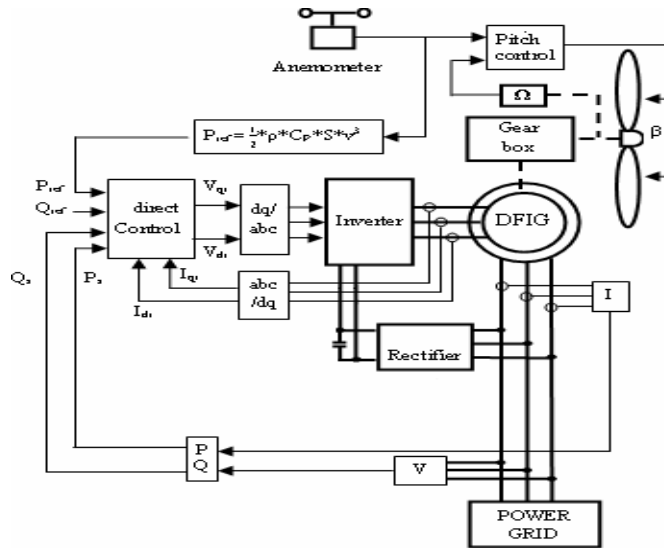


Fig. 4 – Block diagram of the whole system.

The results plotted in the following figures show the powers generated when reference signals are applied. Fig. 5 shows the answers of the system with conventional PI controller, whereas Fig. 6 shows the answers with sliding mode controller.

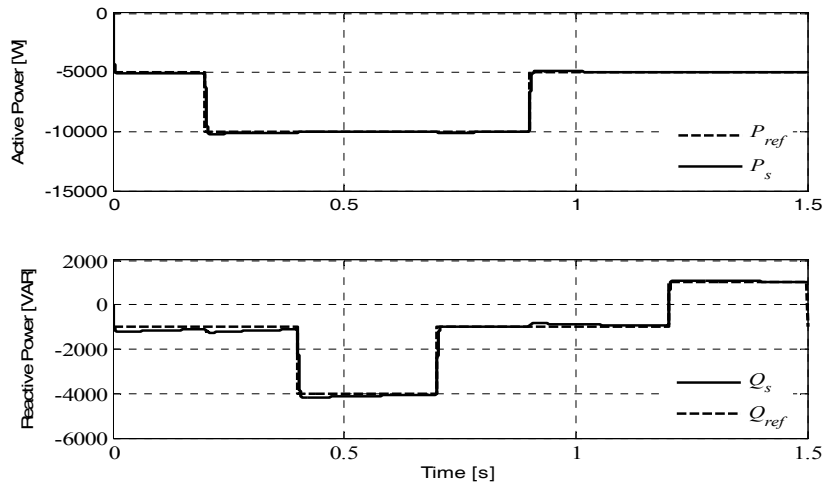


Fig. 5 – System responses with classical PI controller.

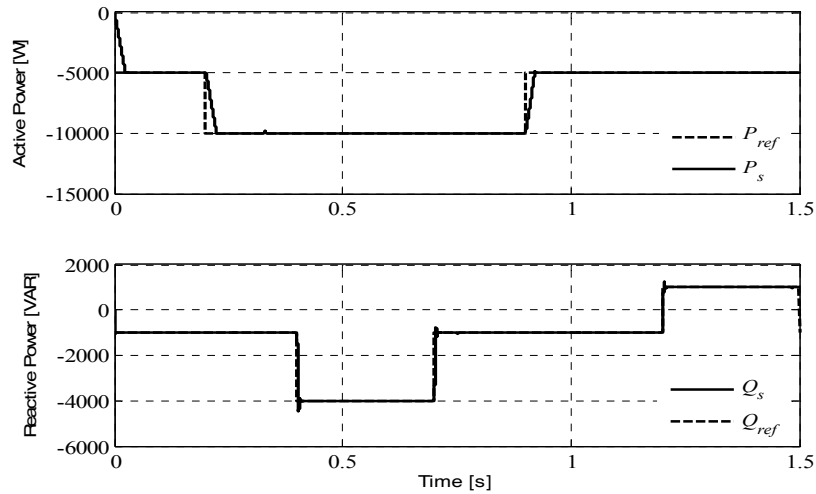


Fig. 6 – System responses with sliding mode controller.

The parameters of the DFIG are $R_s = 0.455 \Omega$, $L_s = 0.07 \text{ H}$, $R_r = 0.19 \Omega$, $L_r = 0.0213 \text{ H}$, $M = 0.034 \text{ H}$.

With PI controller the active and reactive powers follow the desired variables but, it is observed a small coupling effect between the two control axes. In sliding mode control, the answers are without overshoots, no coupling effect, the static error goes to zero, rapid in transient state.

8. CONCLUSION

In this article, it is presented the control of a wind energy conversion system based on a doubly fed induction generator. First, a model of the generator is proposed; then, a control strategy by sliding mode of the asynchronous generator allowing an independent control of the powers is also proposed. The sliding mode controllers of the active and reactive powers are tested. The simulation results show the ameliorated quality of the control based on the controller by sliding mode. Through the response characteristics, we observe good performances even with variations in the reference signal. The output power follows the reference signal without overshoots. The decoupling, the stability and the convergence towards the equilibrium are assured. Furthermore, this regulation presents an algorithm of a very simple robust control and which has the advantage to be easily implantable in a computer control.

Received on June 8, 2010

REFERENCES

1. P.W.Carlin, *The History and State of Art of Variable-Speed Wind Turbine Technology*, NREL/TP500-28607, Février 2001.
2. * * *, <http://www.windpower.org/fr/core.htm>, Association Danoise de l'Industrie éolienne.
3. E. Bossanyi, *Wind Energy Handbook*, New York, Wiley, 2000.
4. Meny Ivan, *Modélisation et réalisation d'une chaîne de conversion éolienne petite puissance*, Laboratoire d'électrotechnique de Montpellier (LEM).
5. B. Multon, *Etat de l'art des aérogénérateurs électriques*, Rapport ECRIN, May 2002.
6. A. Tapia, *Modeling and control of a wind turbine driven doubly fed induction generator*, IEEE Trans. Energy Conversion, **18**, 2, pp. 194–204 (2003).
7. Md. Arifujjaman, *Vector control of a DFIG based wind turbine*, Journal of Electrical & Electronics Engineering, Istanbul, **9**, 2, pp. 1057–1065 (2009).
8. J.M. Carrasco *et al.*, *Power-electronic systems for the grid integration of renewable energy sources*, IEEE Trans. Industrial Electronics, **53**, 4, pp. 1002–1016 (2006).
9. A. Boyette, *Contrôle-commande d'une GADA avec système de stockage pour la production éolienne*, Thèse de Doctorat, Université Henry Poincaré, Nancy I, 2006.
10. Slotine, J.J.E. Li, *Applied nonlinear control*, Prentice Hall, USA, 1998.
11. H. Buhler, *Réglage par mode de glissement*, Presses polytechniques romandes, Lausanne, 1986.